DINAME 2017 - Proceedings of the XVII International Symposium on Dynamic Problems of Mechanics
A. T. Fleury, D. A. Rade, P. R. G. Kurka (Editors), ABCM, São Sebastião, SP, Brazil, March 5-10, 2017

A Comparison Between Parametric and Non-Parametric Methods for Frequency Estimation of Blade Tip Timing Data

Raphael Pereira Spada[1], **Rodrigo Nicoletti**[1]

[1] University of São Paulo, São Carlos School of Engineering Department of Mechanical Engineering, Trabalhador São Carlense Ave. 400, 13566-590 São Carlos, Brazil , raphael.spada@usp.br, rnicolet@sc.usp.br

Abstract: Monitoring blade dynamics is an essential procedure to ensure proper performance of turbomachinery. With the advances in software and hardware over the last decades, the research on blade tip timing (BTT) data analysis, a non-intrusive technique used to measure blade vibrations, has gained momentum. Despite having several advantages over the strain gage monitoring system, the technique has some major issues related to sampling frequency. To attend to this matter, two types of approach have been developed along the years. The first is used to deal exclusively with synchronous vibrations and is based on parametric spectral analysis. The second one is a more recent approach that is capable of dealing with both synchronous and asynchronous excitations and it is based on non-parametric spectral estimation. This paper presents a comparison between the performances of an autoregressive method (parametric) and a minimum variance spectral estimator with multi-sampling (non-parametric), applied to a simulated blade tip timing data, originated by a simple model of a bladed assembly. As a result, it is shown that when dealing with synchronous vibrations the autoregressive method is very reliable, but being a parametric method, it requires some assumptions on the behavior of the structural model, including information on the type of excitation. On the other hand, the non-parametric method was able to perform blind analysis over the data but despite the developments made in the use of this technique, in the context of blade tip timing, some aliasing still occur even in the final spectrum obtained with the multi sampling method. Despite all, the non-parametric approach seems to be the one with most potential of application in real test cases, since no previous knowledge of the structure or assumptions were needed to be made.

Keywords: blade tip-timing, blade vibrations, spectral analysis.

INTRODUCTION

Blades are a fundamental component in turbomachinery and they are often subjected to induced vibrations. For a typical gas turbine, these vibrations are originated through mainly four types of stresses (Carrington, 2002), but the alternating stresses, that are originated by forced response to excitations at multiples of the rotating speed, are the most common cause of high cycle fatigue. These vibrations will diminish the fatigue life and the performance of the blades, which can ultimately lead to catastrophic results. Therefore, carrying on-line vibration monitoring is an intrinsic duty when dealing with turbomachinery.

For a long time strain gages have been the only solution to measuring flexible blade vibrations in rotating machinery. However, the installation of such sensors consists in a very tedious, laborious, costly and time consuming task. This is due specially to the number of blades per stage of the turbine and the requirement of having telemetry or slip rings to acquire the signals. On top of these disadvantages, the sensors can alter the blade dynamics and, more importantly, this monitoring system tends to not be very durable due to the harsh working conditions (Mccarty and Thompson Jr, 1980). In light of these issues, the development of non-intrusive vibration measuring system for rotating blades was boosted.

Describing it in a simple manner, the Blade Tip-Timing (BTT) methodology consists in monitoring blade vibrations by measuring passing times of the blades' tip with static sensors, usually optic, located at the turbine casing. Since the blades are vibrating, the deformation induced will alter these passing times, known as arrival times, when compared with the arrival times of the blades in a non-vibrating referential. This referential can be obtained by placing a sensor on the shaft to measure the actual rotating speed, and by knowing the angular position of the blades, the non-vibrating signal can be generated. This sensor is known as the Once Per Revolution (OPR) sensor.

Despite being a simplistic and straightforward methodology with several advantages over the strain gage measuring procedure, the technique suffers from bad sampling, since the sampling frequency is directly related to the rotating speed and the number of sensors used. To ensure a sampling frequency that attends to the Nyquist criterion, the quantity of sensors involved can be quite substantial. As a result, a significant effort in the BTT scope was devoted to the development and application of techniques capable of identifying vibration properties from a under sampled signal.

Recently, two research fronts on BTT analysis are being used and studied, one that is based on parametric methods that assume some properties of the sampled signal and the other based on non-parametric methods that does not require any assumptions. The works of Carrington *et al.* (2001), Carrington (2002), Gallego-Garrido *et al.* (2002) and Garrido and Dimitriadis(2004) give a good knowledge on the application of parametric methods on BTT context. On the other hand, Beauseroy and Lengelle (2007), Vercoutter *et al.* (2012) and Vercoutter *et al.* (2013) give a good base on non-parametric methods applied in the same context. Both are fundamentally different approaches and, to the knowledge of the authors, these techniques were never evaluated on the same paper, analyzing the same signal.

The goal of this present work is to obtain the frequency of vibration from a signal generated by the forced response of a simple four bladed assembly, modeled as a single degree of freedom for each blade. To reach this goal, a Global Autoregressive (GAR) model and a Minimum Variance Spectral Estimator (MVSE) are applied to the same signal.

SIMULATED MODEL

The simulated model used in this work is equivalent to the one defined by Carrington *et al.* (2001) and presents four degrees of freedom (DOF), one for each blade considered in the assembly. By modeling the system in that manner, only the first bending mode of the blades is taken into consideration and the effects of the rotation are also not considered, such as the centrifugal stiffening and gyroscopic effect of the shaft. The schematic of the model is presented in Fig. 1.

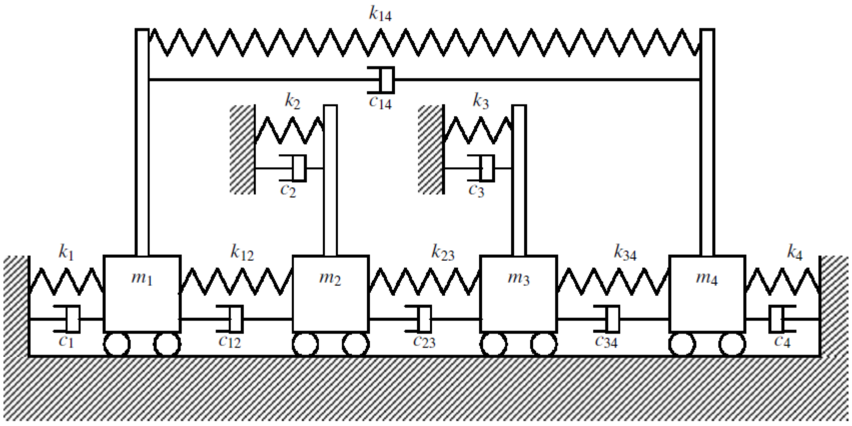

Figure 1 – Schematic of the simulated four bladed assembly. Source:(Carrington *et al.*, 2001).

The system dynamics is described by

$$\mathbf{M}\ddot{\mathbf{x}}(t) + \mathbf{C}\dot{\mathbf{x}}(t) + \mathbf{K}\mathbf{x}(t) = \mathbf{f}(t) \tag{1}$$

in which the mass, stiffness and damping matrices are given by:

$$\mathbf{M} = \begin{bmatrix} m_1 & 0 & 0 & 0 \\ 0 & m_2 & 0 & 0 \\ 0 & 0 & m_3 & 0 \\ 0 & 0 & 0 & m_4 \end{bmatrix}, \tag{2}$$

$$\mathbf{K} = \begin{bmatrix} (k_1+k_{12}+k_{14}) & -k_{12} & 0 & -k_{14} \\ -k_{12} & (k_2+k_{12}+k_{23}) & -k_{23} & 0 \\ 0 & -k_{23} & (k_3+k_{23}+k_{34}) & -k_{34} \\ -k_{14} & 0 & -k_{34} & (k_4+k_{34}+k_{14}) \end{bmatrix}, \tag{3}$$

$$\mathbf{C} = \begin{bmatrix} (c_1+c_{12}+c_{14}) & -c_{12} & 0 & -c_{14} \\ -c_{12} & (c_2+c_{12}+c_{23}) & -c_{23} & 0 \\ 0 & -c_{23} & (c_3+c_{23}+c_{34}) & -c_{34} \\ -c_{14} & 0 & -c_{34} & (c_4+c_{34}+c_{14}) \end{bmatrix}. \tag{4}$$

In the present work it was considered that all blades have the same properties, in a way that when all blades are taken separately they have the same natural frequency of vibration $\omega_n = 30$ Hz, producing a tuned assembly. To achieve this value of frequency the parameters were defined according to Tab. 1. The coupling stiffness and damping (between blades) are defined as 10% of the values of the blade stiffness and damping. With the entire system assembled, the vibration modes of the structure can be identified and they are presented in Tab. 2. It is worth noting that the second and third modes are a double mode due to the symmetric nature of the system.

Table 1 – Model properties.

Property	Value
$m_1 = m_2 = m_3 = m_4 = m$	2 [kg]
$k_1 = k_2 = k_3 = k_4 = k$	71061 [N/m]
$c_1 = c_2 = c_3 = c_4 = c$	7.53 [N.s/m]
ζ	0.01

Table 2 – Natural frequencies of the model.

Mode	Frequency [Hz]
1^{st}	30
2^{nd}	32.9
3^{rd}	32.9
4^{th}	35.5

GLOBAL AUTOREGRESSIVE MODEL

To simulate the signal acquisition through the BTT technique, the simulated model was forced to a synchronous excitation, i.e., a periodic excitation that is an integer multiple of the rotating speed, known as the Engine Order (EO), in each of the masses, as in

$$f(t) = F\sin(2\pi\Omega Et), \tag{5}$$

where F is the magnitude, Ω is the rotating speed in Hz and E is the EO.

Since the rotational effect is not presented on the original model, a virtual rotation in time is created, in a way that the simulated signal is sampled at time instances corresponding to the matching of passing blades with the position of fixed equispaced virtual sensors. The position of the sensors is varied in this study, as it will be shown that it impacts the estimation of frequency. To illustrate the sampled signal, Fig. 2 presents a comparison between the signal sampled with the BTT technique to the original signal for the tip displacement of the first blade, and for the considered model, that is the displacement of the first mass. For the exampled signal, the virtual rotating speed is 10 Hz and the signal has 30 Hz, giving a EO of 3. Considering that the sensors can be displaced around 360º of the circular casing, in a scenario with 3 EO, a full period of the resonance can be observed if the sensors are ranging a $360^o/3 = 120^o$ span. It is seen that in this case the spacing between the first and last probe with respect to the resonance period (PSR) corresponds to 75%, which would mean that in the physical world the first and last probe would be 90º apart, equispaced in-between. In practice, the fact of the EO being utilized to determine the PSR is biased, because the EO, and consequently the resonance frequency, is what is aimed to be estimated, making the real values of PSR only being useful to evaluate the behavior of this methodology.

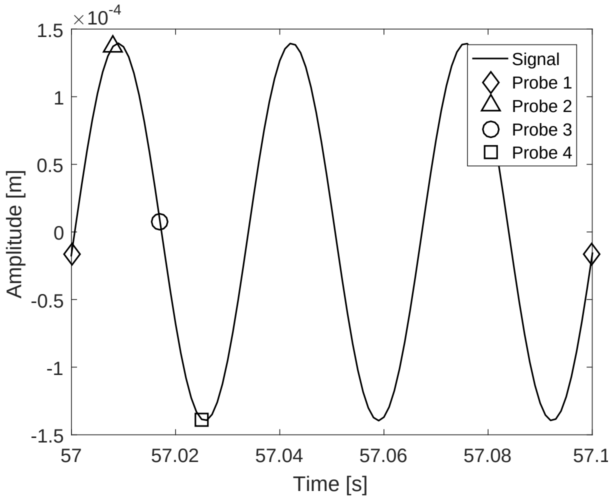

Figure 2 – Example of a BTT sampling with 4 probes and 75% PSR.

The purpose of using the GAR methodology is to identify the first mode of the assembly at 30 Hz and the EO. Considering the Campbell's diagram of Fig. 3, it can be seen the changes in frequencies of the modes when altering the rotating speed. Since the model does not consider rotational effects, the frequencies are not altered with different rotating speeds. This figure is intended to show all the excitations used in the simulation and from it is seen that for the excitations of 1, 2, 3 and 5 EO, the first mode was excited at 1800, 900, 600 and 360 rpm, respectively. The 1 EO case is evaluated because it is a scenario of proper sampling $F_s = 30*4 = 120$ Hz, doubling the Nyquist frequency criterion. The 2 EO case has a sampling frequency exactly equal to the Nyquist frequency $F_s = 60$ Hz. The 3 and 5 EO cases are selected because they have bad sampling frequencies, 40 and 24 Hz, respectively. Considering that the 4 EO case would be intermediary, it was not evaluated.

The formulation of the GAR methodology in the context of BTT was developed in the work of Carrington *et al.* (2001) and to do so, since it is a parametric spectral estimation method, the expected behavior of the signal is firstly defined as a sinusoid of single frequency

$$\hat{x} = A_n\cos(\omega_n t + \varphi_n) + D, \tag{6}$$

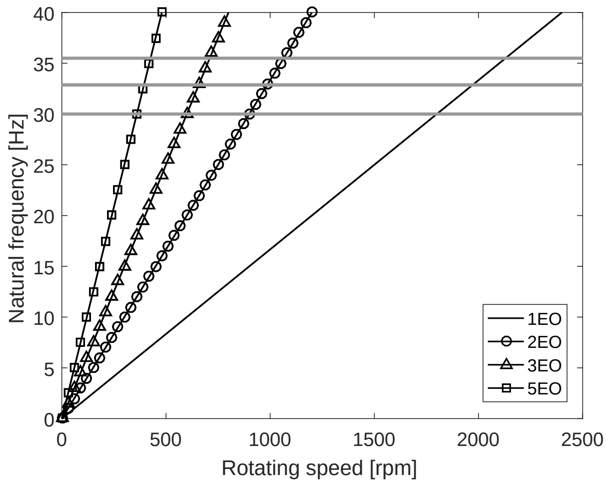

Figure 3 – Campbell's diagram of the assembly.

where A_n, ω_n, and φ_n are the amplitude, natural frequency and phase, respectively. D corresponds to a static offset. This response is solution to

$$\ddot{\hat{x}} + \omega_n^2 \hat{x} = 0. \tag{7}$$

Taking into account that the behavior of the signal is generated that way, a second order autoregressive model is utilized, i.e., the estimation is based on the previous two samples, as in

$$x_j = \sum_{k=1}^{2} a_k x_{(j-k)}, \tag{8}$$

that can be expressed by

$$x_j + a_1 x_{j-1} + a_2 x_{j-2} = 0. \tag{9}$$

Approximating Eq. (7) by a difference equation results in

$$\frac{\hat{x}_{j+1} - 2\hat{x}_j + \hat{x}_{j-1}}{\Delta t_p^2} + \omega_n^2 \hat{x}_j = 0, \tag{10}$$

that can be written as

$$\hat{x}_{j+1} + (\omega_n^2 \Delta t_p^2 - 2)\hat{x}_j + \hat{x}_{j-1} = 0, \tag{11}$$

where Δt_p is the inter-probe time interval.

Now considering that $\hat{x}_j = x_j + D$, then Eq. (11) becomes

$$x_{j+1} + (\omega_n^2 \Delta t_p^2 - 2)x_j + x_{j-1} = D\omega_n^2 \Delta t_p^2. \tag{12}$$

Comparing Eq.(12) to Eq. (9) it is determined that $a_1 = \omega_n^2 \Delta t_p^2 - 2$ and $a_2 = 1$, resulting in the autoregressive model for each blade, considering their static offset.

The autoregressive model is better expressed through matrix format as in

$$\begin{bmatrix} x_3 + x_1 \\ x_4 + x_2 \\ \vdots \\ x_N + x_{N-2} \end{bmatrix} = \begin{bmatrix} x_2 & 1 \\ x_3 & 1 \\ \vdots & \vdots \\ x_{N-1} & 1 \end{bmatrix} \begin{bmatrix} -a_1 \\ D(2 + a_1) \end{bmatrix}, \tag{13}$$

where N indicates the number of sensors. This formulation is the normal autoregressive method for a single revolution and a single blade. It is seen from Eq. (13) that the bare minimum number of sensors is three, but the simple addition of a single sensor enhances the estimation greatly, and that is the reason why this number of probes was used in this work.

To produce the GAR model all blades must be considered through a number of revolutions, resulting in a single a_1

coefficient and consequently a single frequency for all the blades and a D static offset for each blade, as formulated in

$$\begin{bmatrix} x_{1,3,1}+x_{1,1,1} \\ x_{1,4,1}+x_{1,2,1} \\ x_{2,3,1}+x_{2,1,1} \\ x_{2,4,1}+x_{2,2,1} \\ x_{3,3,1}+x_{3,1,1} \\ x_{3,4,1}+x_{3,2,1} \\ x_{4,3,1}+x_{4,1,1} \\ x_{4,4,1}+x_{4,2,1} \\ \vdots \\ x_{1,3,R}+x_{1,1,R} \\ x_{1,4,R}+x_{1,2,R} \\ x_{2,3,R}+x_{2,1,R} \\ x_{2,4,R}+x_{2,2,R} \\ x_{3,3,R}+x_{3,1,R} \\ x_{3,4,R}+x_{3,2,R} \\ x_{4,3,R}+x_{4,1,R} \\ x_{4,4,R}+x_{4,2,R} \end{bmatrix} = \begin{bmatrix} x_{1,2,1} & 1 & 0 & 0 & 0 \\ x_{1,3,1} & 1 & 0 & 0 & 0 \\ x_{2,2,1} & 0 & 1 & 0 & 0 \\ x_{2,3,1} & 0 & 1 & 0 & 0 \\ x_{3,2,1} & 0 & 0 & 1 & 0 \\ x_{3,3,1} & 0 & 0 & 1 & 0 \\ x_{4,2,1} & 0 & 0 & 0 & 1 \\ x_{4,3,1} & 0 & 0 & 0 & 1 \\ \vdots & \vdots & \vdots & \vdots & \vdots \\ x_{1,2,R} & 1 & 0 & 0 & 0 \\ x_{1,3,R} & 1 & 0 & 0 & 0 \\ x_{2,2,R} & 0 & 1 & 0 & 0 \\ x_{2,3,R} & 0 & 1 & 0 & 0 \\ x_{3,2,R} & 0 & 0 & 1 & 0 \\ x_{3,3,R} & 0 & 0 & 1 & 0 \\ x_{4,2,R} & 0 & 0 & 0 & 1 \\ x_{4,3,R} & 0 & 0 & 0 & 1 \end{bmatrix} \begin{bmatrix} -a_1 \\ D_1(2+a_1) \\ D_2(2+a_1) \\ D_3(2+a_1) \\ D_4(2+a_1) \end{bmatrix}, \tag{14}$$

that utilizes four sensors over R revolutions for the four bladed assembly assessed in this paper. In this case the notation $x_{b,s,r}$ stands for the displacement shown by the blade b seen by sensor s at revolution r.

Equation (14) is in the format

$$\mathbf{b} = \mathbf{Y}\mathbf{a}, \tag{15}$$

that is solved in a least-squares manner for the vector $\mathbf{a}$ that contains the information about the signal estimated frequency, resulting in

$$\mathbf{a} = (\mathbf{Y}^T\mathbf{Y})^{-1}\mathbf{Y}^T\mathbf{b}. \tag{16}$$

For continuous time, the coefficient a_1 was defined earlier. By transforming it to discrete time it becomes $a_1 = -2\cos(\omega_n \Delta t_p)$. Therefore, the estimated EO and consequently frequency of vibration can be obtained by

$$EO = \frac{1}{\Omega \Delta t_p} \cos^{-1}\left(-\frac{a_1}{2}\right) \tag{17}$$

and

$$\omega_n = EO\,\Omega, \tag{18}$$

where Ω is the assembly rotating speed.

MINIMUM VARIANCE SPECTRAL ESTIMATOR

According to Vercoutter *et al.* (2012), the MVSE methodology is based on Capon's minimum variance algorithm that works as an adaptive finite impulse response filter bank which allows a sinusoid of frequency f_0 to pass through the filter undistorted while any other frequency component is suppressed. This leads to minimizing the filter variance with the condition that it is subjected to a constraint of passing the frequency of interest f_0 undistorted through the filter. These conditions can be expressed in a minimization problem

$$\min_{\mathbf{a}} \quad \mathbf{a}^H\mathbf{R}\mathbf{a} \qquad\qquad \text{subject to} \quad \mathbf{h}^H(f_0)\mathbf{a} = 1 \tag{19}$$

where $\mathbf{a}$ is the filter coefficients vector and $\mathbf{R}$ is the autocorrelation matrix of the signal. This matrix is assembled from the autocorrelation values of the signal in the format

$$\mathbf{R} = \begin{bmatrix} r_x(0) & r_x(1) & \dots & r_x(N-1) \\ r_x(-1) & r_x(0) & \dots & r_x(N-2) \\ \vdots & \vdots & \ddots & \vdots \\ r_x(1-N) & r_x(2-N) & \dots & r_x(0) \end{bmatrix}, \tag{20}$$

where $r_x(*)$ is the autocorrelation of signal $\mathbf{x}$ with lag $*$.

The solution to the minimization problem leads to

$$\mathbf{a}(f_0) = \frac{\mathbf{R}^{-1}\mathbf{h}(f_0)}{\mathbf{h}^H(f_0)\mathbf{R}^{-1}\mathbf{h}(f_0)}, \tag{21}$$

where

$$\mathbf{h}(f_0) = \begin{Bmatrix} e^{(j2\pi f_0 t_1)} \\ \vdots \\ e^{(j2\pi f_0 t_N)} \end{Bmatrix} \tag{22}$$

and ^{H} denotes the conjugate transpose. With the filter coefficients, the spectral estimation of the signal can be obtained by

$$s(f_0) = \mathbf{x}\mathbf{a}(f_0) \tag{23}$$

From Eq. (21) it is seen that the values of the filter coefficients are dependent on the autocorrelation matrix itself and this matrix is not known beforehand, since the autocorrelation of the signal is based on an infinite horizon approach and for the application only a limited amount of samples are available. To deal with this problem, an iterative algorithm to estimate the autocorrelation matrix was proposed by Greitans (2001) and it is applied in this work. Firstly a rough estimative of the values of the autocorrelation matrix are obtained by

$$\hat{\mathbf{R}}^{\{0\}} = \left|\frac{\mathbf{x}\mathbf{E}^H}{N}\right|^2 \mathbf{E}, \tag{24}$$

where the superscript $^{\{\}}$ indicates the iteration step, $\mathbf{x} = \begin{Bmatrix} x_1 & x_2 & \dots & x_N \end{Bmatrix}$, N is the number of data points and the matrix E is defined as

$$\mathbf{E} = \begin{bmatrix} e^{(-2j\pi f_1 t_1)} & e^{(-2j\pi f_1 t_2)} & \dots & e^{(-2j\pi f_1 t_N)} \\ e^{(-2j\pi f_2 t_1)} & e^{(-2j\pi f_2 t_2)} & \dots & e^{(-2j\pi f_2 t_N)} \\ \vdots & \vdots & \ddots & \vdots \\ e^{(-2j\pi f_M t_1)} & e^{(-2j\pi f_M t_2)} & \dots & e^{(-2j\pi f_M t_N)} \end{bmatrix}, \tag{25}$$

with $\mathbf{f} = \begin{Bmatrix} f_1 & f_2 & \dots & f_M \end{Bmatrix}$ being the desired frequency vector points of the spectral amplitude estimates and $\mathbf{t} = \begin{Bmatrix} t_1 & t_2 & \dots & t_N \end{Bmatrix}$ is the time instances of the N-point data sequence.

The estimated spectral components are computed from

$$\hat{\mathbf{S}}^{\{0\}} = \frac{\mathbf{E}\hat{\mathbf{R}}^{\{0\}^{-1}}\mathbf{x}^T}{\text{diag}(\mathbf{E}\hat{\mathbf{R}}^{\{0\}^{-1}}\mathbf{E}^H)}, \tag{26}$$

that are used to calculate de power spectral density (PSD):

$$\hat{\mathbf{P}}^{\{0\}} = \hat{\mathbf{S}}^{\{0\}^2}. \tag{27}$$

The autocorrelation values of the $\hat{\mathbf{R}}$ matrix are then updated to

$$\hat{R}_{lk}^{\{i+1\}} = \sum_{m=1}^{M} \hat{P}_m^{\{i\}} E_{ml}^* E_{mk}, \tag{28}$$

where l and k are the line and column positions of the matrix, respectively, and the superscript * denotes the conjugate of the complex number.

With the new autocorrelation matrix, the spectral estimates $\hat{\mathbf{S}}^{\{i+1\}}$ can be determined, and consequently the new PSD, that is used again to obtain a new estimative of the autocorrelation matrix. The algorithm is carried out until the following stopping criterion for the PSD is achieved:

$$\Delta = ||\hat{\mathbf{P}}^{\{i+1\}} - \hat{\mathbf{P}}^{\{i\}}|| < 0.01. \tag{29}$$

For the purpose of the application of this technique on a BTT context, an additional approach is used, the multi-sampling methodology, with the goal of reducing the alias obtained in the final spectrum acquired with the MVSE. To do so, two groups of sensors are defined, one with four sensors, the original group, and the other with three, by just inactivating a sensor from the original group. For the MVSE algorithm to work properly, it is critical that the sensors are not equispaced like in the situation of the GAR method. After obtaining the spectrum with the MVSE for the two groups, the inter-spectrum is obtained by the convolution of the spectra

$$S_{inter}(f_i) = S_{group1}(f_i) * S_{group2}(f_i) \tag{30}$$

and it works by enhancing only the frequency components that are present in both spectra, making physical content arise from alias (Vercoutter *et al.*, 2013).

RESULTS

In this section the results for both the GAR and MVSE methodologies are presented.

Global autoregressive model

Table 3 shows the results obtained for four different cases, all of them considering a PSR of 75% and four different EO exciting the first mode (30 Hz). From the results, it can be seen that the technique extracted the real frequency of the signal with great accuracy, even in situations severely undersampled, such as the 5 EO case, where the average sampling is $f_s = \Omega * N_s = 24$ Hz, less than half the Nyquist frequency of 60 Hz.

Table 3 – GAR results.

Real		Estimated	
EO	Ω	EO	ω_n
1	1800 rpm	1.00	30.01 Hz
2	900 rpm	2.00	29.99 Hz
3	600 rpm	3.05	30.54 Hz
5	360 rpm	5.00	29.99 Hz

Despite the great results obtained, the PSR was left constant throughout the test cases. To understand the effect of the positioning of the sensors around the casing of the turbine, the PSR was varied from 15% up to 150% for the two more undersampled test cases of 3 and 5 EO. As seen in Fig. 4, for low values of PSR the method does not estimate the signal frequency correctly and it is identified that in the range from 60% up to 145% PSR the method is able to recover the true frequency of the signal.

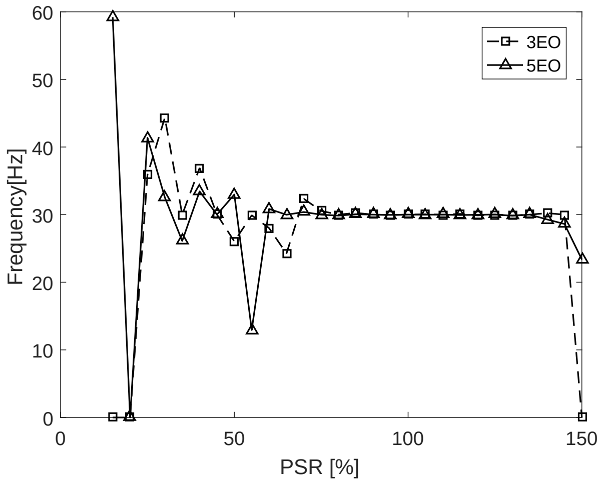

Figure 4 – Estimated values of frequency varying the PSR for the 3 and 5 EO cases.

Minimum variance spectral estimator

For the MVSE methodology, two scenarios were considered, one with a 3 EO excitation and a second with 5 EO, exciting the first mode of the assembly. The reason for this is that the 1 EO and 2 EO excitation gives a scenario where the Nyquist frequency criterion is attended, given that the sampling frequency on these situations are, respectively, 120 and 60 Hz. In those scenarios a simple Discrete Fourier Transform (DFT) would be sufficient to identify the signal spectrum.

For the 3 EO case, Fig. 5 shows the results obtained with MVSE from the original group of four sensors. It can be seen a lot of frequency components that are not really present in the signal, since it is a sinusoid of single frequency of 30 Hz. On Fig. 6 it can be seen from the spectrum obtained with three sensors, that artifacts arise from different frequencies in different magnitudes. From the inter-spectrum of Fig. 7 it is seen that the artifacts of the spectrum have vanished, but there are still aliased peaks at multiples of the rotating speed, as seen in 10 and 20 Hz. Still, the strongest component of the signal is identified at 30 Hz, with the maximum aliased peak having 20% of the magnitude of the real signal frequency.

The same observations can be made about the results from the 5 EO test case, from Fig. 8 to Fig. 10, the difference is that the aliased peaks occur at multiples of 6 Hz, the rotating speed in this case. Also, it is more difficult to distinguish the real frequency component from the aliased peaks, since there are peaks at 6 and 24 Hz of 57% relative intensity.

As stated before, the MVSE has an advantage over the GAR method, as it can also identify asynchronous vibrations and it is also capable of analyzing a signal that has more than one frequency. To evaluate that, a new test case is defined, with two excitations occurring at the same time, at the rotating speed of 500 rpm, exciting the first and fourth mode of the assembly at 30 and 35 Hz. Figure 11 shows the inter-spectrum from the asynchronous test case. It can be seen now that both components of 30 and 35 Hz arise from the aliased peaks that reach a maximum of 19% of the real components

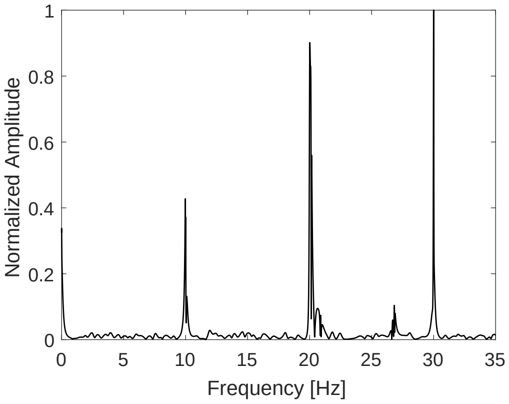

Figure 5 – Normalized spectrum obtained by the MVSE with 4 sensors for the 3 EO case.

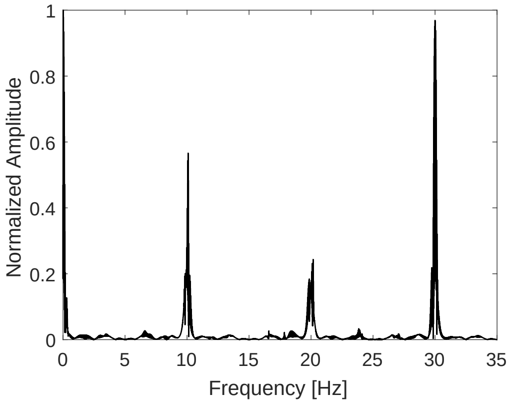

Figure 6 – Normalized spectrum obtained by the MVSE with 3 sensors for the 3 EO case.

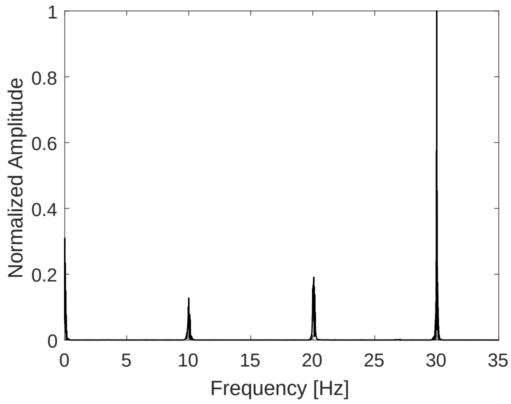

Figure 7 – Inter-spectrum of the two groups for the 3 EO case.

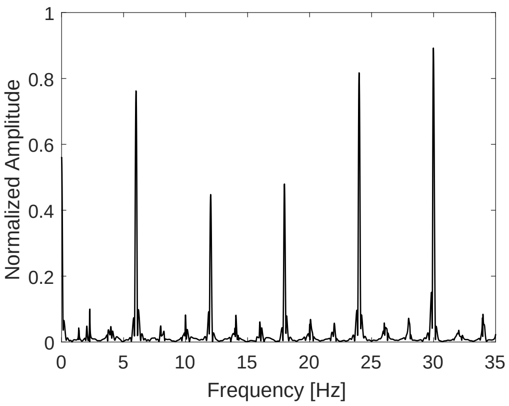

Figure 8 – Normalized spectrum obtained by the MVSE with 4 sensors for the 5 EO case.

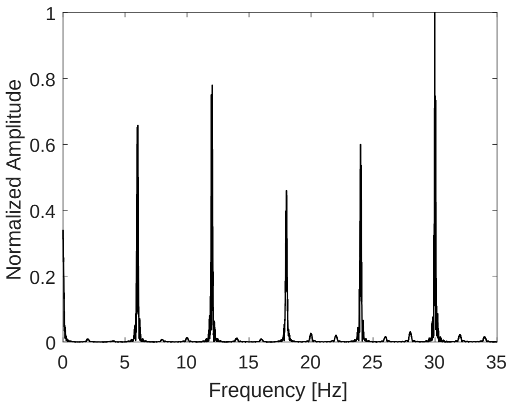

Figure 9 – Normalized spectrum obtained by the MVSE with 3 sensors for the 5 EO case.

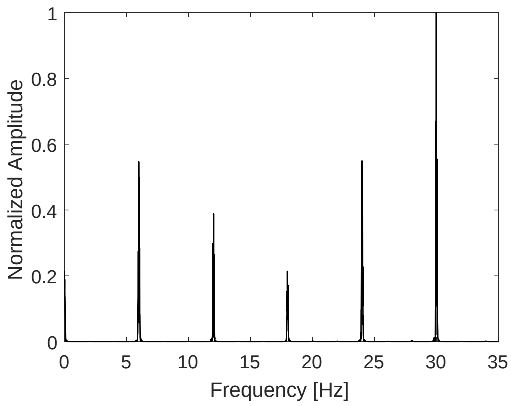

Figure 10 – Inter-spectrum of the two groups for the 5 EO case.

amplitude.

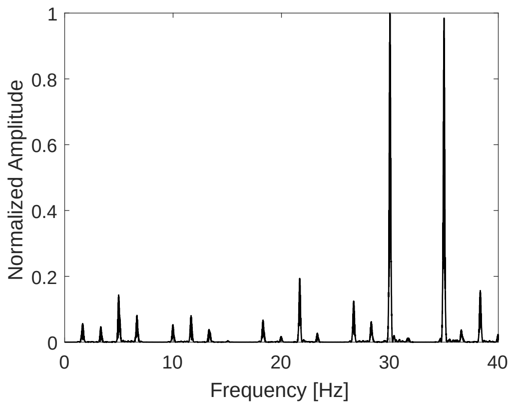

Figure 11 – Inter-spectrum of the two groups considering the asynchronous case with two excitations.

CONCLUSIONS

This paper presented an application of the GAR and MVSE methodologies on the same simulated model of a bladed assembly to identify the advantages and disadvantages of each technique when applied to a BTT context. Firstly, the GAR approach presented great results, retrieving the correct frequency of the signal for the test cases analyzed, but some assumptions were needed to be made, such as the type of excitation (GAR can only perform for synchronous excitation) and the quantity of frequencies presented in the signal (it can only identify one frequency). Despite presenting great results for a 75% PSR, it was shown that the positioning of the sensors were an integral part for obtaining correct results with the methodology. By varying the PSR for different simulations, it was identified a PSR range where the methodology can be used effectively. Considering that the information of PSR is not available beforehand, from a practical standpoint finding the PSR range that is suitable to obtain correct results can be impractical, since the positioning of the physical sensors should be altered until a stability of the response were achieved.

Regarding the MVSE approach, it was shown that no assumptions were needed to be made on the behavior of the system, or the type of excitation involved. Also, the MVSE alone cannot produce reliable results due to aliasing on the obtained spectrum. To remedy that, the multi-sampling approach was applied, reducing significantly the alias of the combined spectrum. In addition to this, the technique was also capable of working in a asynchronous excitation test with two simultaneous frequencies of excitation. The best results were achieved in this scenario, where the remaining aliased peaks were lower than 20% of the correct identified frequencies, in magnitude.

In conclusion, it was shown that the MVSE algorithm, when combined with the multi-sampling technique, can be a powerful tool of identifying the spectrum of BTT generated signals, since it does not require any previous knowledge of the system dynamics. However, even with the application of a multi-sampling approach to reduce aliasing on the final spectrum, it still persists, although in a smaller magnitude. The efforts in future works should be in further reducing the aliasing produced in the final spectrum and evaluating the effects of considering the rotational dynamics of the blades.

ACKNOWLEDGMENTS

This project was supported by the Brazilian research foundation CNPq (Conselho Nacional de Desenvolvimento Científico e Tecnológico).

REFERENCES

Beauseroy, P., Lengellé, R., 2007, "Nonintrusive turbomachine blade vibration measurement system", Mechanical Systems and Signal Processing, vol. 21, n.4, pp. 1717-1738.

Carrington, I.B., Wright, J.R., Cooper, J.E.,Dimitriadis, G., 2001, "A comparison of blade tip timing data analysis methods", Proceedings of the Institution of Mechanical Engineers, Part G: Journal of Aerospace Engineering, vol. 215, n.5, pp. 301-312.

Carrington, I.B., 2002, "Development of blade tip timing data analysis techniques", PhD thesis, University of Manchester, Manchester, United Kingdom.

Gallego-Garrido, J., Dimitriadis, G., Wright, J.R., 2002, "Development of a multiple modes simulator of rotating bladed assemblies for blade tip-timing data analysis", Proceedings of the 2002 International Conference on Noise and Vibration Engineering, Leuven, Belgium, pp. 1437-1446.

Garrido, J.G., Dimitriadis, G., 2004, "Multiple Frequency Analysis Methods for Blade Tip-Timing Data Analysis", Proceedings of the ASME 7th Biennial Conference on Engineering Systems Design and Analysis, Manchester, United Kingdom, pp. 75-83.

Greitans, M.,2001, "Multiband signal processing by using nonuniform sampling and iterative updating of autocorrelation matrix", Proceedings of the 2001 International Conference on Sampling Theory and Application, pp. 85-89.

McCarty, P.E., Thompson Jr, J.W., 1980, "Development of a Noninterference Technique for Measurement of Turbine Engine Compressor Blade Stress", No. AEDC-TR-79-78, Arnold Engineering Development Center.

Vercoutter, A., Berthillier, M., Talon, A., Burgardt, B., Lardies, J., 2012, "Estimation of turbomachinery blade vibrations from tip-timing data", Proceedings of the 10th International Conference on Vibrations in Rotating Machinery, London, United Kingdom, pp. 233-245.

Vercoutter, A., Lardies, J., Berthillier, M., Talon, A., Burgardt, B., 2013, "Improvement of compressor blade vibrations spectral analysis from tip timing data: aliasing reduction", Proceedings of the ASME Turbo Expo 2013: Turbine Technical Conference and Exposition, San Antonio, United States, vol. 7A, pp. V07AT26A006-V07AT26A006.

RESPONSIBILITY NOTICE

The authors are the only responsible for the material included in this paper.